Available online at www.sciencedirect.com
ScienceDirect
Control Engineering Practice 15 (2007) 1–16
CONTROL ENGINEERING PRACTICE
www.elsevier.com/locate/conengprac

Structured Set Membership identification of nonlinear systems with application to vehicles with controlled suspension ☆

Mario Milanese*, Carlo Novara

Dipartimento di Automatica e Informatica, Politecnico di Torino, Corso Duca degli Abruzzi 24, 10129 Torino, Italy

Received 25 June 2004; accepted 27 January 2006
Available online 31 March 2006

Abstract

This paper considers an iterative algorithm for the identification of structured nonlinear systems. The systems considered consist of the interconnection of a MIMO linear systems and a MIMO nonlinear system. The considered interconnection structure can represent as particular cases Hammerstein, Wiener or Lur'e systems. A key feature of the proposed method is that the nonlinear subsystem may be dynamic and is not assumed to have a given parametric form. In this way the complexity/accuracy problems posed by the proper choice of the suitable parametrization of the nonlinear subsystem are circumvented. Moreover, the simulation error of the overall model is shown to be a nonincreasing function of the number of algorithm iteration. The effectiveness of the algorithm is tested on the problem of identifying a model for vertical dynamics of vehicles with controlled suspensions from both simulated and experimental data.

Keywords: Structured identification; Nonlinear systems; Controlled suspension vehicles

1. Introduction

In the paper, the problem of using data and physical information in the identification of complex nonlinear systems is investigated. Consider a discrete time MIMO system represented by a regression function $f_o = [f_o^1, \ldots, f_o^q]$ describing the time evolution of system output as

$$\begin{aligned} y_{t+1}^i &= f_o^i(w_t^i), \quad i = 1, \ldots, q, \\ w_t^i &= [y_t^i, \ldots, y_{t-n_y}^i, \\ &\qquad u_t^1 \ldots u_{t-n_1}^1, \ldots, u_t^m, \ldots, u_{t-n_m}^m] \in \Re^{n_i}. \end{aligned} \tag{1}$$

Identification aim is to find estimates $\hat{f}$ of f_o from a set of noise corrupted measurements $\tilde{y}_t^i$ and $\tilde{w}_t^i$, $i = 1, \ldots, q, t = 1, 2, \ldots, T$ of outputs y_t^i and of regressors w_t^i, possibly minimizing some measure of the identification error $f_o - \hat{f}$. Because of finiteness of data, no finite bound or confidence interval can be derived for the identification error if no further information is available on $f_o(w)$. This information is typically given by assuming that it belongs to some parametric family $f(w, \theta)$ of functions. When possible, first principle laws are used to derive equations describing the evolution of the variable of interest, where the functional forms of involved nonlinear functions are known, depending on some unknown parameters θ. In other situations, due to the fact that the laws are too complex or not sufficiently known, this is not possible or not convenient and a black-box approach is taken, considering that f_o belongs to a suitably chosen parametrized set of functions $f(w, \theta) = \sum_{i=1}^{r} \alpha_i \sigma_i(w, \beta_i)$, $\beta_i \in \Re^q$, where $\theta = [\alpha, \beta]$ and the σ_i's are given functions, e.g. piece-wise linear, polynomial, sigmoidal, wavelet, etc. (Haber & Unbehauen, 1990; Isermann, Ernst, & Nelles, 1997; Narendra & Mukhopadhyay, 1997; Sjöberg et al., 1995). In both cases, physical or black-box modeling, the problem is reduced to estimating the parameters θ from data. This task may be performed by minimizing some suitable functional, as done e.g. in

☆This research was supported in part by Ministero dell'Università e della Ricerca Scientifica e Tecnologica under the Project "Robustness techniques for control of uncertain systems" and by GM-FIAT World Wide Purchasing Italia under the Project "Modeling of vehicles vertical accelerations".

*Corresponding author. Tel.: +39 011 5647020; fax: +39 011 5647099.
E-mail addresses: mario.milanese@polito.it (M. Milanese), carlo.novara@polito.it (C. Novara).

0967-0661/$ - see front matter © 2006 Elsevier Ltd. All rights reserved.
doi:10.1016/j.conengprac.2006.01.001

prediction error methods, which exhibit important statistical properties (Bauer & Ninness, 2002; Ljung & Caines, 1979). However, several problems may arise. The functional to be minimized may result in most cases not convex and trapping in local minima may occur, causing serious accuracy problems even in case of exact modeling, i.e. that $f_o(w) = f(w, \theta^o)$ for some "true" θ^o. Indeed, in general both first principle laws or black-box model selection procedures can give only approximate modeling of the involved phenomena, i.e. not completely correct information is provided to the identification procedure, since $f_o(w) \neq f(w, \theta)$, $\forall \theta$. The incorrect part of the assumed information may counteract the positive effects induced on identification accuracy by the correct part. Evaluating the overall balance of these two effects on the identification error, though actively investigated in the last decade for the case of linear systems (Chen & Gu, 2000; Milanese, Norton, Piet Lahanier, & Walter, 1996; Partington, 1991), is a largely open problem for nonlinear systems.

These considerations suggest the interest in identification methods able to account for different kinds of knowledge about the system, able to provide information which may be to a large extent considered correct. In many applications, this can be provided by information on the physical interconnection structure of the system to be identified, allowing its decomposition in subsystems, connected through unmeasured signals. Typical cases considered in the literature are Hammerstein, Wiener and Lur'e systems, consisting of two subsystems, a linear dynamic one and a nonlinear static one, connected in cascade or feedback form (Bai, 2002, 2003; Billings & Tsang, 1990; Crama & Shoukens, 2001; Lang, 1997). Among the many approaches proposed in the literature for the identification of such classes of systems, iterative algorithms have been proposed (see e.g. Narendra & Gallman, 1966; Rangan, Wolodkin, & Poolla, 1995; Stoica, 1981; Vörös, 1999) based on the fact that if the interconnecting signals are known, the identification problem reduces to the identification of each subsystems from their input–output data. The guesses on the interconnecting signal are then iteratively adapted on the base of the identified submodel at each iteration. Though their convergence properties are not completely understood (Crama & Shoukens, 2001; Narendra & Gallman, 1966; Rangan et al., 1995; Stoica, 1981; Vörös, 1999) these algorithms proved to give satisfactory results in many simulated and real problems.

In this paper we propose an iterative algorithm, based on the same principle, able to deal with more complex interconnection structures which may arise in practical applications, where the nonlinear subsystems may be dynamic.

A key feature of the method is that the nonlinear dynamic subsystems are not supposed to have a given parametric model. In this way the above discussed problems posed by the proper choice of a suitable parametrization and the drawbacks related to the effects of approximate modeling are circumvented. Moreover, the simulation error of the overall model is shown to be a nonincreasing function of iterations. Indeed, the algorithm may converge in few iterations to very satisfactory estimates even for quite rough initializations, as shown in the presented example, related to the identification of the vertical dynamics of vehicles with controlled suspensions. Two sets of data are used. The first set is composed of simulated data, thus allowing direct comparisons of identified subsystems and connecting signal with the "true" ones generating the data. The second set consists of experimental data acquired on a real car, thus showing that the proposed structured identification algorithm may prove to give quite good results in nontrivial real applications.

2. Structured experimental modeling

In the paper it is considered that the system to be identified, using information on its physical interconnection, can be represented by the decomposition structure of Fig. 1.

All the signals u, y, v may be multivariable. Submodels M_1 and M_2 are dynamic MIMO discrete time systems, one linear and the other nonlinear. The problem is to identify M_1 and M_2, supposing that noise corrupted measurements $\tilde{u} = [\tilde{u}_1, \ldots, \tilde{u}_T]$ and $\tilde{y} = [\tilde{y}_1, \ldots, \tilde{y}_T]$ of input and output sequences are available, but the interconnecting sequence $v = [v_1, v_2, \ldots]$ is unknown.

Note that this structure allows to represent widely studied classes of models such as: Hammerstein models, where M_1 is a static nonlinearity $v(t) = f(u(t))$ not depending on y and M_2 is linear dynamic; Wiener models, where M_2 is a static nonlinearity $y(t) = f(v(t))$ and M_1 is linear dynamic with transfer function from y to v equal to zero; Lur'e models, where M_1 is a static nonlinearity $v(t) = f(u(t) - v(t))$ and M_2 is linear dynamic. Indeed, more complex structures can be represented as well, e.g. the one of Fig. 6, arising in modeling vehicles vertical dynamics.

Assuming parametric forms $M_1(\theta_1)$ and $M_2(\theta_2)$ for the two subsystems, estimates of θ_1, θ_2 can be obtained e.g. by prediction error methods. Even if linear parametrizations are adopted for M_1 and M_2, the overall optimization problem is not convex, possibly leading to poor identification results because of trapping in local minima. Alternative iterative procedures have been proposed for the identification of Hammerstein or Wiener models, based on the fact that if interconnecting signal v is known, the problem reduces to estimation of $M_1(\theta_1)$ and $M_2(\theta_2)$ from

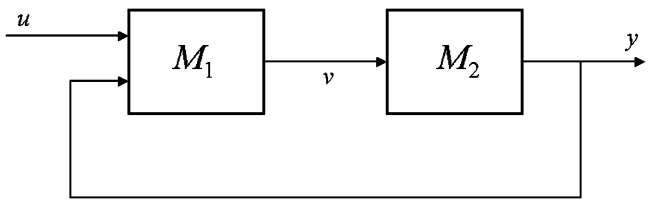

Fig. 1. Structure decomposition.

their input–output data. Then, the guesses on the interconnecting signal v are iteratively adapted on the base of the identified submodel at each iteration (see e.g. Narendra & Gallman, 1966; Rangan et al., 1995; Stoica, 1981; Vörös, 1999).

An iterative identification scheme based on the same principle is here proposed for the general structure of Fig. 1, where the nonlinear subsystem may be dynamic and no assumption on functional form of the related regression function is made.

A model M is represented in regression form by its regression function f. Just for the sake of simplicity, consider that M_1 is nonlinear, while M_2 is linear. Then, M_1 is represented by the nonlinear regression:

$$v_{t+1} = f(v_t, v_{t-1}, \ldots, v_{t-n_v}, y_t, y_{t-1}, \ldots, y_{t-n_y}, u_t, u_{t-1}, \ldots, u_{t-n_u})$$

and M_2 is represented by the linear regression:

$$y_{t+1} = a_o y_t + a_1 y_{t-1} + \cdots + a_{n_y} y_{t-n_y} + b_o v_t + b_1 v_{t-1} + \cdots + b_{n_v} v_{t-n_v}.$$

The output sequence of a model M driven by an input sequence u is indicated as $M[u]$. The model relating u and y in Fig. 1 is denoted as $M(M_1, M_2)$, i.e. $y = M(M_1, M_2)[u]$.

Let the sequences $u = [u_1, \ldots, u_T]$ and $y = [y_1, \ldots, y_T]$ be known, while $v = [v_1, \ldots, v_T]$ is unknown. Consider a partition of known data: $y = [y^e, y^v]$, $u = [u^e, u^v]$.

Structured identification algorithm

- Initialization:
  - Get an initial guess $M_2^{(o)}$ for M_2 and set $M_1^{(o)} = 0$
  - Set k = 1
- Iteration k:

(1) Compute a sequence $v^{(k)}$ such that $M_2^{(k-1)}[v^{(k)}] \approx y^e$
(2) Identify a nonlinear regression model $\tilde{M}_1^{(k)}$ using u^e and y^e as input sequences and $v^{(k)}$ as output sequence
(3) Identify a linear model $\tilde{M}_2^{(k)}$ using $\tilde{v}^{(k)} = \tilde{M}_1^{(k)}[u^e, y^e]$ as input sequence and y^e as output sequence
(4) Compute $\alpha^* = \arg\min_{\alpha \in R^2} J(y^v - y_\alpha^{(k)})$ where:
$J(y^v - y_\alpha^{(k)}) = \|y^v - y_\alpha^{(k)}\|_2^2$
$y_\alpha^{(k)} = M(M_1^\alpha, M_2^\alpha)[u^v]$
$M_1^\alpha = M_1^{(k-1)} + \alpha_1(\tilde{M}_1^{(k)} - M_1^{(k-1)})$
$M_2^\alpha = M_2^{(k-1)} + \alpha_2(\tilde{M}_2^{(k)} - M_2^{(k-1)})$
(5) Set $M_1^{(k)} = M_1^{\alpha^*}$, $M_2^{(k)} = M_2^{\alpha^*}$, $k = k+1$ and return to step 1

In step 1, if a stable right inverse of $M_2^{(k)}$ exists, $v^{(k)} = (M_2^{(k)})^{-1}[y^e]$ could be chosen. If a right inverse of $M_2^{(k)}$ does not exists or is not stable, $v^{(k)}$ can be computed as $v^{(k)} = M_2^\dagger[y^e]$ where $M_2^\dagger$ is an approximate stable inverse of $M_2^{(k)}$ computed by solving the following H_∞ optimization problem:

$$M_2^\dagger = \arg \min_{Q \in \mathscr{H}_\infty} \|[1 - M_2^{(k)} Q] W\|_\infty,$$

where W is a low pass filter chosen on the basis of the spectral features of measured signals and of noise affecting such measurements. Even in case a stable right inverse of $M_2^{(k)}$ exists, the use of $M_2^\dagger$ instead of the exact inverse is preferable, in order to avoid unduly amplification of the effects of noise outside the spectral band of measured signals.

In step 2, the nonlinear Set Membership (NSM) method of Milanese and Novara (2004) can be used in order to circumvent the above discussed drawbacks related to the choice of a suitable parametric forms of the regression function f_2 representing M_2 and by the effects of the resulting approximation. Indeed, the NSM method does not assume any parametric form for f_2, but only a bound on its gradient. A brief outline of the method is reported in Section 3.

Note that choosing $\alpha = 1$ and using parametric models estimated by prediction error method, the algorithm reduces to classical iterative algorithms proposed for Hammerstein and Wiener models (see e.g. Narendra & Gallman, 1966; Stoica, 1981; Vörös, 1999). However, in such cases the nonincreasing behavior of the simulation error may not take place, caused not only by the above discussed problems of nonconvexity of prediction error functional and approximate modeling, but also by the fact that minimization of prediction error does not imply minimization of simulation error (see e.g. Milanese & Novara, 2003).

The next result shows that the iterative identification algorithm proposed in this paper is such that the simulation error $J^*(k)$ is not increasing for increasing number of algorithm iterations.

Proposition 1. *Let* $J^*(k) = \min_{\alpha \in R^2} J(y^v - y_\alpha^{(k)})$. *Then*

$$J^*(k+1) \leqslant J^*(k), \quad \forall k.$$

Proof. Clearly

$$J^*(k) = \min_{\alpha \in R^2} J(y^v - y_\alpha^{(k)}) = J(y^v - y_{\alpha^*(k)}^{(k)}),$$
$$y_{\alpha^*(k)}^{(k)} = M(M_1^{\alpha^*(k)}, M_2^{\alpha^*(k)})[u^v],$$

where the notation $\alpha^*(k)$ is used to evidence the dependence of α^* on k. On the other hand:

$$y_{\alpha=0}^{(k+1)} = M(M_1^{(k)}, M_1^{(k)})[u^v].$$

Since $M_1^{(k)} = M_1^{\alpha^*(k)}$ and $M_2^{(k)} = M_2^{\alpha^*(k)}$, it follows: $y_{\alpha=0}^{(k+1)} = M(M_1^{\alpha^*(k)}, M_1^{\alpha^*(k)})[u^v] = y_{\alpha^*(k)}^{(k)}$. Then

$$J(y^v - y_{\alpha=0}^{(k+1)}) = J(y^v - y_{\alpha^*(k)}^{(k)}) = J^*(k).$$

Taking the minimum over α shows that:

$$J^*(k+1) = \min_{\alpha \in R^2} J(y^v - y_\alpha^{(k+1)}) \leqslant J^*(k). \qquad \square$$

3. Set membership identification of nonlinear systems

In this section the main concepts and results of the NSM identification method (Milanese & Novara, 2004) used in step 2 are briefly recalled.

Consider that a set of noise corrupted data $\tilde{Y}_T = [\tilde{y}_{t+1},\ t = 1,2,\ldots,T]$ and $\tilde{W}_T = [\tilde{w}_t,\ t = 1,2,\ldots,T]$ generated by (1) is available. For the sake of notational simplicity the case $q = 1$ is considered. Then

$$\tilde{y}_{t+1} = f_o(\tilde{w}_t) + d_t, \quad t = 1,2,\ldots,T, \tag{2}$$

where the term d_t accounts for the fact y_{t+1} and w_t are not exactly known.

The aim is to derive an estimate $\hat{f}$ of f_o from available measurements $(\tilde{Y}_T, \tilde{W}_T)$, i.e. $\hat{f} = \phi(\tilde{Y}_T, \tilde{W}_T)$. The operator ϕ, called identification algorithm, should be chosen to give small (possibly minimal) L_p error $\|f_o - \hat{f}\|_p$, where $\|f\|_p \doteq [\int_W |f(w)|^p\, dw]^{1/p}$, $p \in [1,\infty)$ and $\|f\|_\infty \doteq \text{ess-sup}_{w \in W} |f(w)|$ and W is a given bounded set in $\Re^n$.

Whatever algorithm ϕ is chosen, no information on the identification error can be derived, unless some assumptions are made on the function f_o and the noise d. The typical approach in the literature is to assume a finitely parametrized functional form for f_o (linear, bilinear, neural network, etc.) and statistical models on the noise (Haber & Unbehauen, 1990; Isermann et al., 1997; Narendra & Mukhopadhyay, 1997; Sjöberg et al., 1995). In the NSM approach, different and somewhat weaker assumptions are taken, not requiring the selection of a parametric form for f_o, but related to its rate of variation. Moreover, the noise sequence $D_T = [d_1, d_2, \ldots, d_T]$ is only supposed to be bounded.

Prior assumptions on f_o:
$f_o \in K \doteq \{f \in C^1(W) : \|f'(w)\| \leqslant \gamma,\ \forall w \in W\}$.

Prior assumptions on noise:
$D_T \in \mathscr{D} \doteq \{[d_1,\ldots,d_T] : |d_t| \leqslant \varepsilon_t,\ t = 1,2,\ldots,T\}$.

Here, $C^1(W)$ is the class of continuously differentiable functions on the set W, $f'(w)$ denotes the gradient of $f(w)$ and $\|x\| \doteq \sqrt{\sum_{i=1}^n x_i^2}$ is the Euclidean norm.

A key role in this Set Membership framework is played by the feasible systems set, often called "unfalsified systems set", i.e. the set of all systems consistent with prior information and measured data.

Definition 1. The feasible systems set FSS_T is

$$FSS_T \doteq \{f \in K : |\tilde{y}_{t+1} - f(\tilde{w}_t)| \leqslant \varepsilon_t,\ t = 1,2,\ldots,T\}. \tag{3}$$

The feasible systems set FSS_T summarizes all the information on the mechanism generating the data that is available up to time T. If prior assumptions are "true", then $f_o \in FSS_T$, an important property for evaluating the accuracy of identification.

As typical in any identification theory, the problem of checking the validity of prior assumptions arises. The only thing that can be actually done is to check if prior assumptions are invalidated by data, evaluating if no system exists consistent with data and assumptions, i.e. if FSS_T is empty. Indeed the fact that the priors are consistent with the present data, i.e. $FSS_T \neq \emptyset$, does not exclude that they may be not consistent with future data. However, it is usual to introduce the concept of prior assumption validation as follows.

Definition 2. Prior assumptions are considered validated if $FSS_T \neq \emptyset$.

Necessary and sufficient condition for checking the assumptions validity are given by the following result. Let us define the functions:

$$\begin{aligned} \overline{f}(w) &\doteq \min_{t=1,\ldots,T} (\overline{h}_t + \gamma \|w - \tilde{w}_t\|), \\ \underline{f}(w) &\doteq \max_{t=1,\ldots,T} (\underline{h}_t - \gamma \|w - \tilde{w}_t\|), \end{aligned} \tag{4}$$

where $\overline{h}_t \doteq \tilde{y}_{t+1} + \varepsilon_t$ and $\underline{h}_t \doteq \tilde{y}_{t+1} - \varepsilon_t$.

Theorem 1.

(i) $\overline{f}(\tilde{w}_t) \geqslant \underline{h}_t,\ t = 1,2,\ldots,T$
is necessary condition for prior assumptions to be validated.

(ii) $\overline{f}(\tilde{w}_t) > \underline{h}_t,\ t = 1,2,\ldots,T$
is sufficient condition for prior assumptions to be validated.

Proof. See Milanese and Novara (2004). $\square$

The validation Theorem 1 and prior information on the system can be jointly used for assessing the values of the constants γ and ε_t appearing in the assumptions on function f_o and on noise d_t such that sufficient condition holds (see Milanese & Novara, 2004).

The functions $\overline{f}(w)$ and $\underline{f}(w)$ allow also to solve the problem of finding the smallest interval guaranteed to include $f_o(w)$. In fact, provided that prior assumptions hold:

$$\inf_{f \in FSSF_T} f(w) \leqslant f_o(w) \leqslant \sup_{f \in FSS_T} f(w), \quad \forall w \in W. \tag{5}$$

Thus, $\sup_{f \in FSS_T} f(w)$ and $\inf_{f \in FSSF_T} f(w)$ are the tightest upper and lower bounds of $f_o(w)$ and are called *optimal bounds*.

The following theorem shows that the optimal bounds are actually given by $\overline{f}(w)$ and $\underline{f}(w)$.

Theorem 2.

$$\overline{f}(w) = \sup_{f \in FSS_T} f(w),$$
$$\underline{f}(w) = \inf_{f \in FSSF_T} f(w).$$

Proof. See Milanese and Novara (2004). □

For given estimate, $\phi(FSS_T) = \hat{f}$, the related L_p error $\|f_o - \hat{f}\|_p$ cannot be exactly computed, but its tightest bound is given by $\|f_o - \hat{f}\|_p \leqslant \sup_{f \in FSS_T} \|f - \hat{f}\|_p$. This motivates the following definition of the identification error, often indicated as guaranteed error.

Definition 3. The identification error of $\hat{f} = \phi(FSS_T)$ is

$$E[\phi(FSS_T)] \doteq \sup_{f \in FSS_T} \|f - \hat{f}\|_p.$$

Looking for algorithms that minimize the identification error, leads to the following optimality concepts.

Definition 4. An algorithm ϕ^* is called optimal if

$$E[\phi^*(FSS_T)] = \inf_{\phi} E[\phi(FSS_T)] = r_I.$$

The quantity r_I, called *radius of information*, gives the minimal identification error that can be guaranteed by any estimate based on the available information up to time T.

The next result shows that the algorithm:

$$\phi_c(FSS_T) = f_c \doteq \tfrac{1}{2}(\underline{f} + \overline{f})$$

is optimal for any L_p norm and that the corresponding minimal identification error can be actually computed.

Theorem 3. *For any $L_p(W)$ norm, with $p \in [1, \infty]$:*

(i) *The identification algorithm $\phi_c(FSS_T) = f_c$ is optimal.*
(ii) $E(f_c) = \tfrac{1}{2}\|\overline{f} - \underline{f}\|_p = r_I = \inf_\phi E[\phi(FSS_T)]$.

Proof. See Milanese and Novara (2004). □

We conclude this section by summarizing the main features of the NSM method, and by comparing them to the main features of the most common identification methods in the literature.

- The NSM method does not assume to know the functional form of nonlinear regression function, in contrast with most methods, which assume that it belongs to a finitely parametrized family. Thus, the method does not require extensive searches of such functional form and reduces the effects of modeling errors due to the use of approximate forms.
- The NSM method does not require to solve an iterative optimization problem. At the contrary, most of parametric methods are based on the prediction error method, which requires the iterative minimization of a quadratic error function. In several cases, such as neural and neuro-fuzzy networks, the minimization problem is nonconvex. This gives rise to possible deteriorations in accuracy due to trapping in local minima.
- The noise is assumed to be bounded in the NSM context. Standard approaches use instead statistical assumptions such as stationarity, uncorrelation, etc. The validity of such assumptions is difficult to be reliably checked and anyway is lost in presence of approximate modeling.

On the basis of these theoretical features, it is expected that models obtained by means of the proposed method may have good performance and exhibit good robustness versus imprecise knowledge of involved nonlinearities and of noise properties.

4. Identification of controlled suspension vehicles: simulation data

Models of vehicles vertical dynamics are very important tools in the automotive field, especially in view of the increasing diffusion of controlled suspension systems (Krtolica & Hrovat, 1992; Lu & DePoyster, 2002). Indeed, accurate models may allow efficient tuning of control algorithms in computer simulation environment, thus significantly reducing the expensive in-vehicle tuning effort.

In this section, unstructured and structured identification procedures are performed on simulated data obtained by the half-car model shown in Fig. 2. The main variables describing the model are:

- p_{rf} and p_{rr}: front and rear road profiles.
- i_{sf} and i_{sr}: control currents of front and rear suspensions.
- a_{cf} and a_{cr}: front and rear chassis vertical accelerations.
- p_{cf} and p_{cr}: front and rear chassis vertical positions.
- p_{wf} and p_{wr}: front and rear wheels vertical positions.
- F_{cf} and F_{cr}: forces applied to chassis by front and rear suspensions.
- F_{wf} and F_{wr}: forces applied to front and rear wheels by tires.

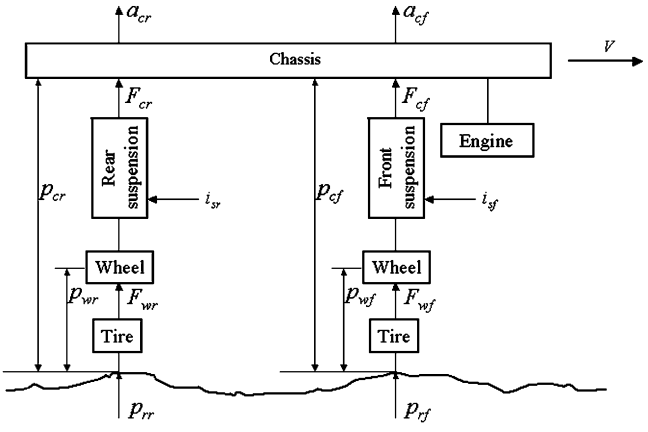

Fig. 2. The half-car model.

The chassis, the engine and the wheels are simulated as rigid bodies. The vehicle is assumed to travel in a constant speed $V = 60\,\mathrm{km/h}$. The following nonlinear characteristic has been assumed for suspensions:

$$F_{c*}(t) = K_s \Delta p_s(t) + F_s(\Delta v_s(t), i(t)),$$

where * stands for f or r, F_{c*} is the suspension force, $\Delta p_s = p_{w*} - p_{c*}$ and $\Delta v_s = \dot{p}_{w*} - \dot{p}_{c*}$ are the differences of position and velocity at the extremes of suspension, i is the control current, $K_s = 17\,200\,\mathrm{N/m}$, $F_s(\Delta v_s, i)$ is shown in Fig. 3a for the two extreme values $i = 0$ and $1.6\,\mathrm{A}$. The following static nonlinear characteristic has been assumed for tires:

$$F_{w*}(t) = F_e(\Delta p_w(t)) + \beta_w \Delta v_w(t),$$

where F_{w*} is the tire force, $\Delta p_w = p_{r*} - p_{w*}$ and $\Delta v_w = \dot{p}_{r*} - \dot{p}_{w*}$ are the differences of position and velocity at the extremes of tire, $\beta_w = 10\,000\,\mathrm{Ns/m}$ and $F_e(\Delta p_w)$ is shown in Fig. 3b.

The half-car model, called for short "true system", has been implemented in Simulink in order to obtain data simulating a possible experimental setup, characterized by type of exciting input, experiment length, variables to be measured and accuracy of sensors.

It is considered that the road profile $p_{rf}(t)$ is known, that $p_{rr}(t) = p_{rf}(t - \ell/V)$, where ℓ is the distance between front and rear wheels, that currents $i_{sf}(t)$ and $i_{sr}(t)$ can be measured with a precision of 3.75% and that variables $a_{cf}(t)$, $a_{cr}(t)$ can be measured with a precision of 5%.

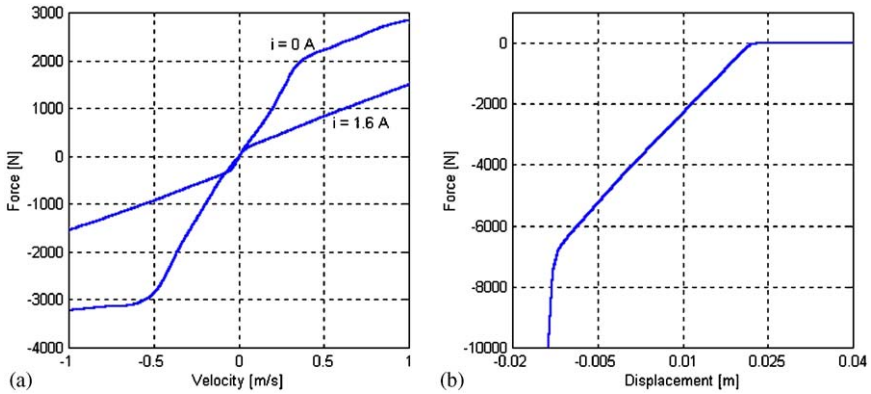

Fig. 3. (a) Force-velocity characteristic F_s of suspension. (b) Force–displacement characteristic F_e of tires.

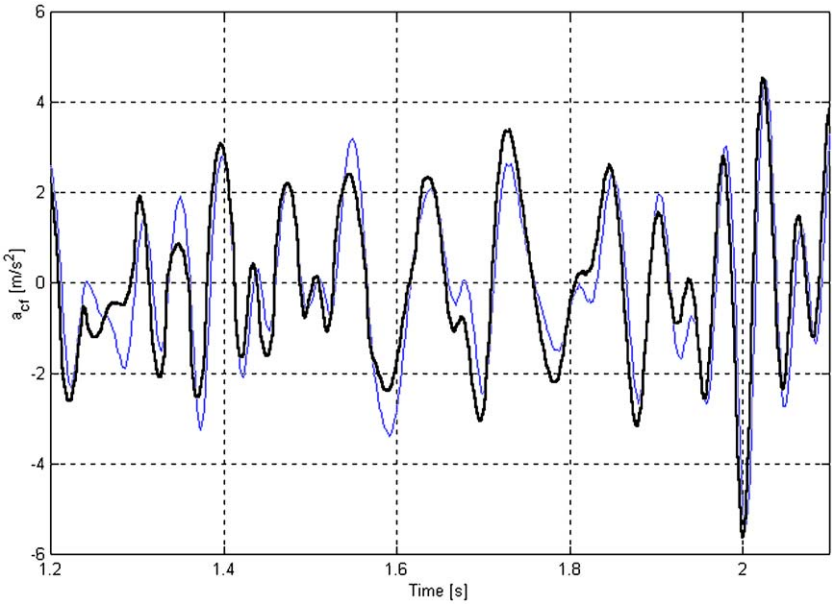

Fig. 4. Simulation data: front chassis accelerations: "true" (bold line), NSMU model (thin line).

A data set has been generated from "true system" simulation, for a period of 24 s, using a random profile with amplitude <4 cm. The data set consists of the values of p_{rf}, p_{rr}, i_{sf}, i_{sr}, a_{cf} and a_{cr} recorded with a sampling time of $\tau = \frac{1}{512}$ s. The sequence of each measured variables is composed of 12 280 samples. The values of a_{cf} and a_{cr} have been corrupted by uniformly distributed noises of relative amplitude 5% and the values of i_{sf} and i_{sr} have been corrupted by uniformly distributed noises of relative amplitude 3.75%. The data set related to the first 20 s, called estimation data set, has been used for models identification. The data set related to the last 4 s, called validation data set, has been used to test the simulation accuracy of identified models.

Discrete time models with four inputs and two outputs, relating front and rear chassis accelerations to the road profile and control currents at the sampling times, have been identified from the estimation data set. In particular, an overall nonlinear model, indicated as NSMU (nonlinear set membership unstructured), not using information on system structure, has been identified using the Set Membership approach.

The model is of form (1) with $q = 2$, $m = 4$, $y_t^1 = a_{cf}(t\tau)$, $y_t^2 = a_{cr}(t\tau)$, $u_t^1 = p_{rf}(t\tau)$, $u_t^2 = p_{rr}(t\tau)$, $u_t^3 = i_{sf}(t\tau)$ and $u_t^4 = i_{sr}(t\tau)$. Models with values of n_y, n_1, n_2, n_3, n_4 up to 10 have been identified and the best one has been chosen, having $n_y = 8$, $n_1 = 3$, $n_2 = 3$, $n_3 = 1$, $n_4 = 1$.

The simulation results of such a model has been tested on the validation data set. Because of space limitations, results related to the front acceleration are reported, but the ones related to the rear acceleration are similar.

In Fig. 4, a portion of "true" data and of the ones obtained by the identified NSMU model are reported. The root mean square simulation error on the validation data set is reported in Table 1.

In order to check if better results could be obtained by using alternative unstructured methods, a model has been identified using the neural networks toolbox of Matlab. Several one-hidden-layer neural networks with sigmoidal basis functions and with number of neuron ranging from 3 to 20 have been trained on the estimation set and the best estimated model, having 6 neurons, has been chosen and called NNU. The simulation results on the validation data set reported in Table 1 suggest the evidence that using only the available data without further information on the system structure, no more accurate models could be obtained. The structured identification approach of Section 2 is then used. Considering its physical structure, the half-car model can be represented by the block diagram of Fig. 5.

The block CE represents the behavior of chassis and engine. Since for usual road profiles the chassis pitch angle are small ($<5-6^\circ$), this block can be considered linear. The blocks S_f and S_r represent the behavior of front and rear suspension dampers and springs. These blocks are the main sources of nonlinearities in the system, mainly due to the significant nonlinearities of dampers, see Fig. 3a. The blocks W_f and W_r represent the inertial behavior of front and rear wheels and unsprung masses. These blocks are linear. The

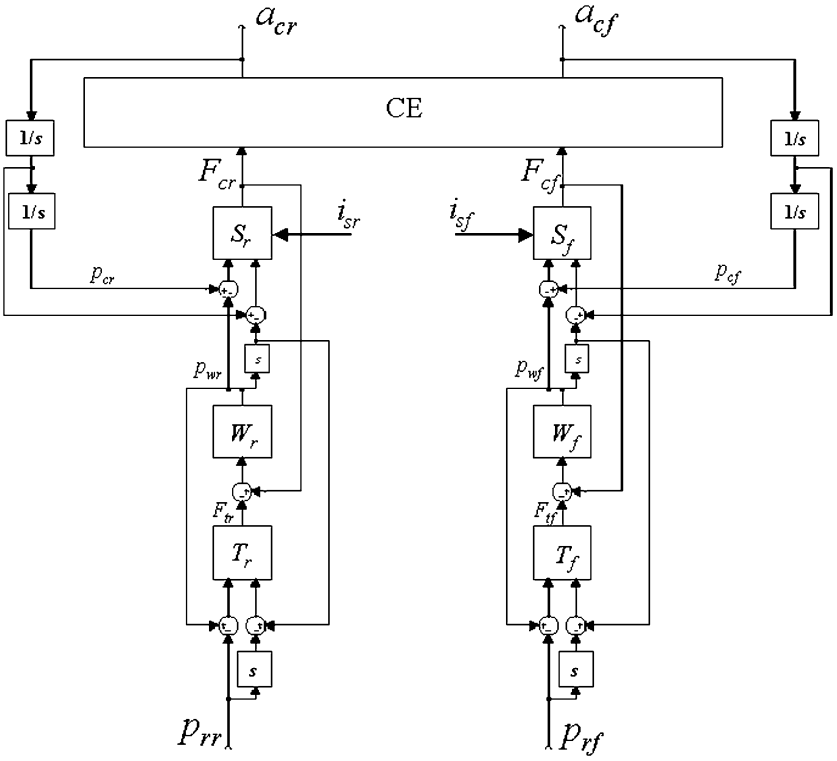

Fig. 5. Block diagram of half-car model.

blocks T_f and T_r represent the behavior of front and rear tires. These blocks also are nonlinear, see Fig. 3b.

The block diagram of Fig. 5 can be represented in a more compact form by the block diagram of Fig. 6. In this form, the half-car model is represented as a generalized Lur'e system, consisting of the linear MIMO system CE, connected in a feedback form with the two nonlinear dynamic systems SWT_f and SWT_r, representing the overall behavior of front and rear suspensions, wheels and tires.

This decomposition structure can be recast in the form of Fig. 1 with the following positions:

$$u = \begin{bmatrix} p_{rr} \\ p_{rf} \\ i_{sr} \\ i_{sf} \end{bmatrix}, \quad y = \begin{bmatrix} a_{cr} \\ a_{cf} \end{bmatrix}, \quad v = \begin{bmatrix} F_{cr} \\ F_{cf} \end{bmatrix}.$$

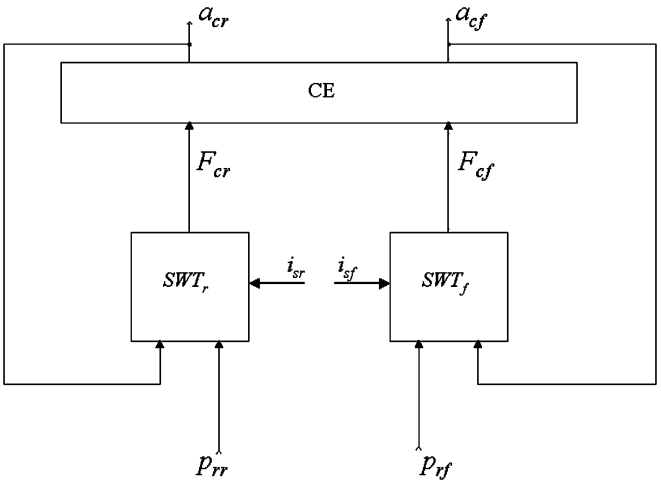

Fig. 6. Generalized Lur'e form of half-car model.

Clearly $M_2 = CE$ and represents the behavior of chassis and engine, while subsystem M_1 is composed of the two nonlinear dynamic systems SWT_f and SWT_r, representing the overall behavior of front and rear suspensions, wheels and tires.

Based on this decomposition structure, the iterative identification algorithm of Section 2 has been applied. The overall identified model relating u and y identified at the end of iteration k is denoted $\text{NSMS}^{(k)}$.

The initial guess for CE required at the initialization step has been obtained from the laws of motion, assuming chassis and engine as a unique rigid body, leading to a 2×2 transfer matrix with constant elements. Indeed, the "true" 2×2 transfer matrix has elements which are transfer functions of order 4, see Fig. 7 where the Bode plots of elements (1,1) of these transfer matrices are reported. It can be noted that this initial model error is relevant, giving large errors ($\simeq 100\%$) in the initial estimates of forces F_{cf} and F_{cr}, see Fig. 8. This under-modeling is intentionally introduced, in order to show that despite of this rough initialization, the algorithm converges in few iterations to a quite good solution.

In step 2, discrete time nonlinear models of SWT_f and SWT_r are identified using the NSM approach of Milanese and Novara (2004). The models are of the form:

$$v_{t+1} = f(v_t, \ldots, v_{t-n_v}, y_t, \ldots, y_{t-n_y}, u_t^1, \ldots, u_{t-n_1}^1, u_t^2, \ldots, u_{t-n_2}^2)$$

with $v_t = F_{c*}(t\tau)$, $y_t = a_{c*}(t\tau)$, $u_t^1 = p_{r*}(t\tau)$, $u_t^2 = i_{s*}(t\tau)$, where * stands for f or r. Models with values of n_v, n_y, n_1 and n_2 between 1 and 6 have been identified and the best one has been chosen, having $n_v = 2$, $n_y = 3$, $n_1 = 3$, $n_2 = 1$.

In step 3, the model of CE is obtained identifying linear output error (OE) models by means of the Matlab

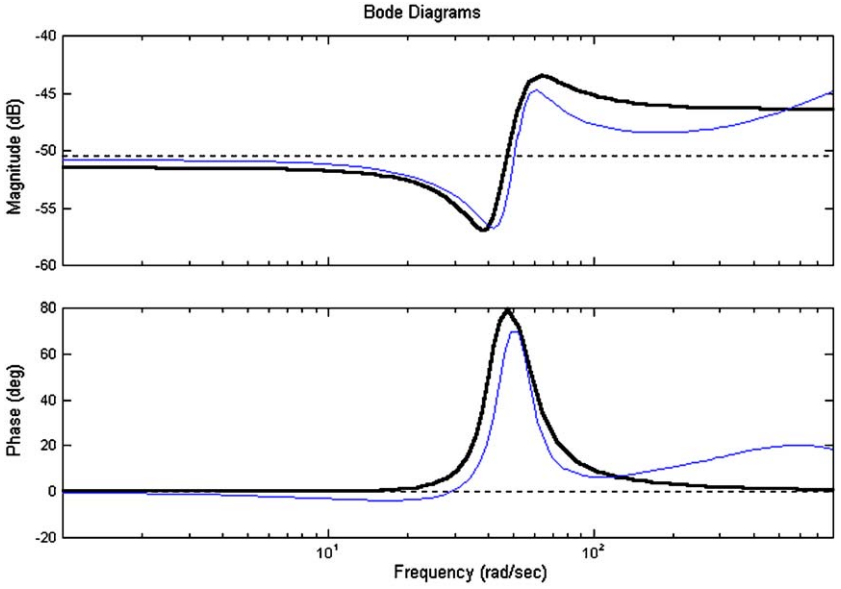

Fig. 7. Simulation data: bode plots of $CE(1,1)$: "true" (bold line), initial model (dashed line), model at iteration 2 (thin line).

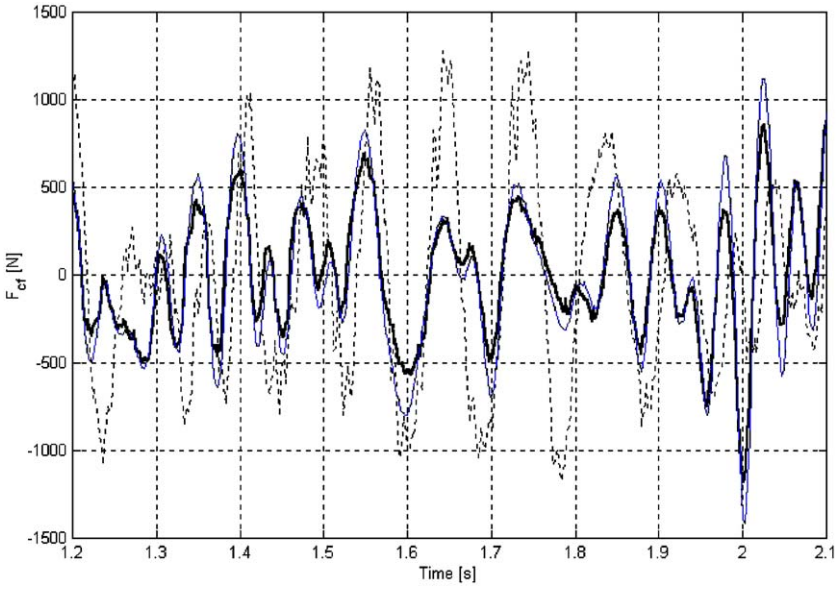

Fig. 8. Simulation data: forces applied to chassis from suspensions: "true" (bold line), estimate at iteration 1 (dashed line), estimate at iteration 2 (thin line).

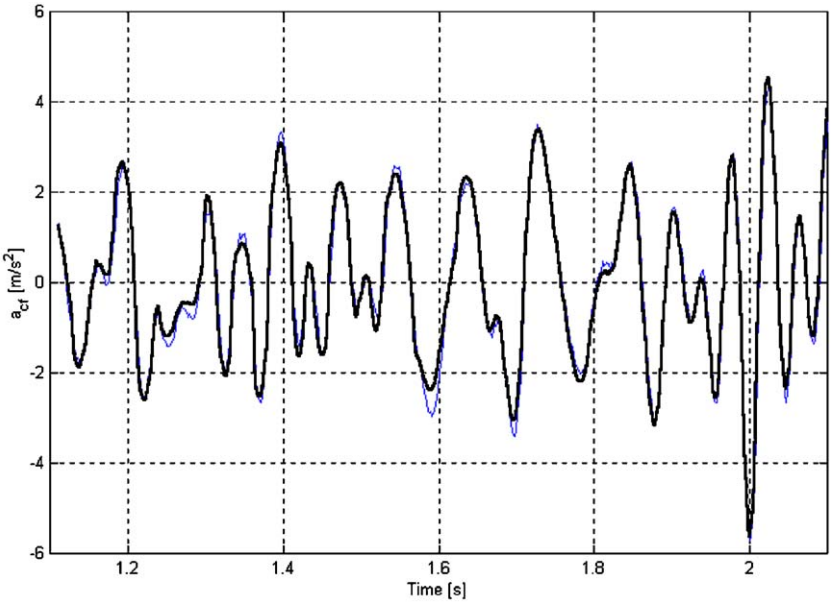

Fig. 9. Simulation data: front chassis accelerations: "true" (bold line), NSMS$^{(2)}$ model (thin line).

Identification Toolbox, of the following form:

$$y_{t+1} = a_o y_t + \cdots + a_{n_y} y_{t-n_y} + b_o v_{t+1} + \cdots + b_{n_v} v_{t-n_v}$$

with $v_t = [F_{cf}(t\tau), F_{cr}(t\tau)]$, $y_t = [a_{cf}(t\tau), a_{cr}(t\tau)]$. Several orders have been tested and the best results have been obtained by an $OE(6,6,0)$ model.

The results derived by the NSMS$^{(k)}$ models identified at iterations $k = 1, 2$ are now compared with "true" data on the testing data set.

In Fig. 7 the elements (1,1) of the "true" transfer matrix CE, of the initial guess and of transfer matrix identified at the 2nd iteration are reported. In Fig. 8 "true" forces applied to chassis by suspensions and the ones estimated at the 1st and 2nd iteration are shown. In Fig. 9 "true" front

Table 1
Simulation data: root mean square front chassis acceleration errors on the validation data set

Model	NSMU	NNU	NSMS$^{(1)}$	NSMS$^{(2)}$
RMSE	0.656	0.660	0.502	0.208

acceleration and the ones estimated by NSMS$^{(2)}$ model are shown for a portion of validation data. In Table 1 the root mean square simulation errors between "true" and estimated front accelerations are reported.

It can be noted that, though the initialization of iterative algorithm is (intentionally) quite crude, after two iterations the estimates of transfer matrix CE and of forces F_{c*} are significantly improved, reflecting in significant improvements of identification accuracy evaluated by chassis accelerations errors. A third iteration has been also performed, but no significant decrease of errors have been obtained. Finally, it can be noted that a significant improvement in identification accuracy over the unstructured identification methods has been obtained. In fact, the *RMSE* errors provided by the unstructured models NNU and NSMU are about 300% greater than the *RMSE* error provided by the structured model NSMS$^{(2)}$.

5. Identification of controlled suspension vehicles: experimental data

In this section identification is performed from experimental data measured on a "four-poster" test bench of a segment C car, equipped with a continuous dampers control. Vertical displacements at tires are imposed, related to different types of road profiles at different constant speeds and front and rear chassis accelerations, wheels accelerations, and control currents of the dampers are measured. These measurements are obtained from the onboard accelerometers, needed by the continuous dampers control system. The tests for the acquisitions of experimental data were performed in the Fiat—Elasis Research Center in Pomigliano d'Arco (Italy) on a C-segment prototype vehicle, equipped with controlled dampers and a CDC-Skyhook (continuous damping control) system. The CDC-Skyhook system is characterized by the following control settings:

- Constant hard (CH): The dampers currents are on average zero, giving the maximum dampening effect.
- Hard (H): The dampers are controlled with current modulated by the CDC-Skyhook control unit according to a "sporting" calibration.
- Soft (S): The dampers are controlled with current modulated by the CDC-Skyhook control unit according to a "comfort" calibration.
- Constant soft (CS): The dampers currents are on average maximum, giving the minimum dampening effect.

The tests for the model identification were performed on a "four-poster" MTS test bench, specifically designed for vibration analysis of complete vehicles, see Fig. 10. This test bench is composed of four plates, which are vertically driven by hydraulic pistons, in order to simulate given road profiles.

For each test, the variables which are used for the identification of the model were measured by means of the original CDC-Skyhook sensors: 2 vertical accelerometers on the chassis, positioned at the front left and right suspension top mount; 1 vertical accelerometer on the chassis, positioned at the rear right suspension top mount.

Furthermore, the test bench provides the position measures of the 4 plates. The pistons of the test bench were driven using experimental data from road tests on specific road profiles. The used road profiles (see Table 2)

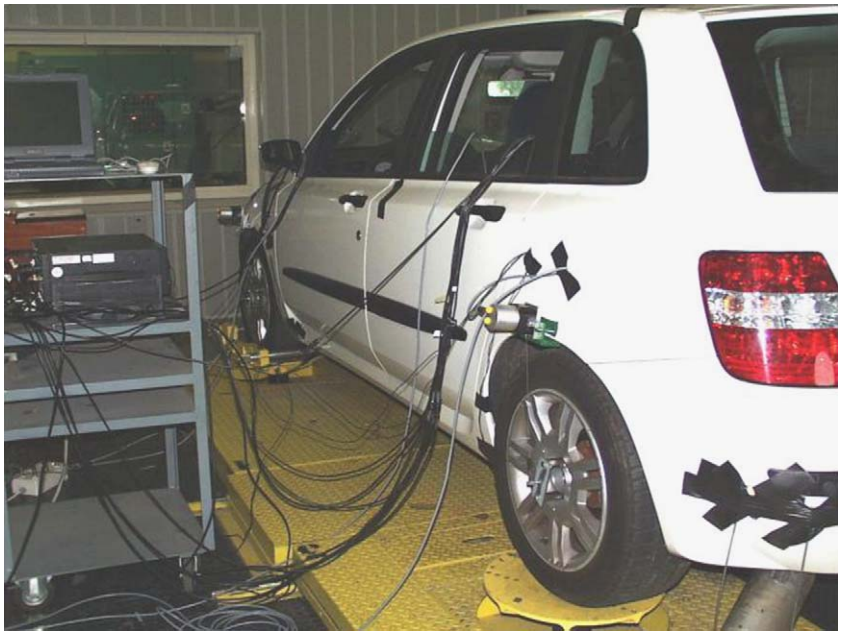

Fig. 10. Car on the "four-poster" test bench.

Table 2
Road profiles and Skyhook settings used for data acquisition

Road profile	Speed (km/h)	Skyhook setting	Length (s)
Random	60	CH	14
Random	60	H	14
Random	60	S	14
Random	60	CS	14
English track	60	CH	14
English track	60	H	14
English track	60	S	14
English track	60	CS	14
Short back	30	S	14
Motorway	140	CH	14
Motorway	140	CS	14
Pavé	40	CH	14
Drain well	30	S	14

are symmetric with respect to the longitudinal axis of the vehicle and are among the ones used for the on-road tuning of the CDC control system. These road profiles were chosen since they allow to test different dynamic conditions of the vehicle, in terms of frequencies and amplitudes:

- Random: random road.
- English track: road with irregularly spaced holes and bumps.
- Short back: impulse road.
- Motorway: level road.
- Pavé track: road with small amplitude irregularities.
- Drain well: negative impulse road.

The vehicle speed during the on-road acquisition is associated at each road profile. Such speed was also used to determine the delay between the front and rear plates displacements and was also fed to the CDC-Skyhook system for its own algorithms. The sampling frequency is 512 Hz for all the signals.

The complete data set, consisting of 93 184 data, has been partitioned as follows:

- *Identification set*: The data corresponding to the first 7 s of each acquisition. This set has been used for model identification.
- *Testing set*: The data corresponding to seconds from 7 to 14 of each acquisition. This set has been used for testing the accuracy of identified models on data not used for identification.

Since the considered road profiles are symmetric with respect to the longitudinal axis of the vehicle, the half-car decomposition structure of Fig. 6 has been considered, which, as shown in the previous section, can be recast in the form of Fig. 1.

Based on this decomposition structure, the iterative identification algorithm of Section 2 has been applied. The overall identified model relating u and y identified at the end of iteration k is denoted NSMS$^{(k)}$.

The initial guess for CE required at the initialization step has been obtained from the laws of motion, assuming a rigid chassis interacting with the engine through linear spring and dumper.

In step 2, discrete time nonlinear models of SWT_f and SWT_r are identified using the Set Membership approach of Milanese and Novara (2004). The models are of the form:

$$v_{t+1} = f(v_t, \ldots, v_{t-n_v}, y_t, \ldots, y_{t-n_y}, u_t^1, \ldots, u_{t-n_1}^1, u_t^2, \ldots, u_{t-n_2}^2)$$

with $v_t = F_{c*}(t\tau)$, $y_t = a_{c*}(t\tau)$, $u_t^1 = p_{r*}(t\tau)$, $u_t^2 = i_{s*}(t\tau)$, where * stands for f or r. Models with values of n_v, n_y, n_1 and n_2 between 1 and 6 have been identified and the best one has been chosen, having $n_v = 1$, $n_y = 2$, $n_1 = 2$, $n_2 = 2$.

In step 3, the model of CE is obtained identifying linear OE models by means of the Matlab Identification Toolbox, of the following form:

$$y_{t+1} = a_o y_t + \cdots + a_{n_y} y_{t-n_y} + b_o v_{t+1} + \cdots + b_{n_v} v_{t-n_v}$$

with $v_t = [F_{cf}(t\tau), F_{cr}(t\tau)]$, $y_t = [a_{cf}(t\tau), a_{cr}(t\tau)]$. Several orders have been tested and the best results have been obtained by an $OE(6,6,0)$ model.

In Table 3 the root mean square errors ($RMSE$) of front and rear chassis accelerations obtained by models NSMS$^{(1)}$

Table 3
Experimental data: root mean square chassis acceleration errors on the testing data set

Model	*RMSE* (front)	*RMSE* (rear)
NSMS$^{(1)}$	2.85	3.53
NSMS$^{(2)}$	0.71	0.86

Table 4
Experimental data: root mean square chassis acceleration errors obtained by model NSMS$^{(2)}$ on the testing data set

Road profile	Skyhook setting	*RMSE* (front)	*RMSE* (rear)
Random	CH	1.24	1.54
Random	H	0.59	0.65
Random	S	0.55	0.59
Random	CS	0.67	0.68
English track	CH	1.50	1.93
English track	H	1.03	1.21
English track	S	1.04	1.20
English track	CS	1.08	1.49
Short back	S	0.39	0.52
Motorway	CH	0.35	0.46
Motorway	CS	0.31	0.39
Pavé	CH	0.85	1.07
Drain well	S	0.55	0.63

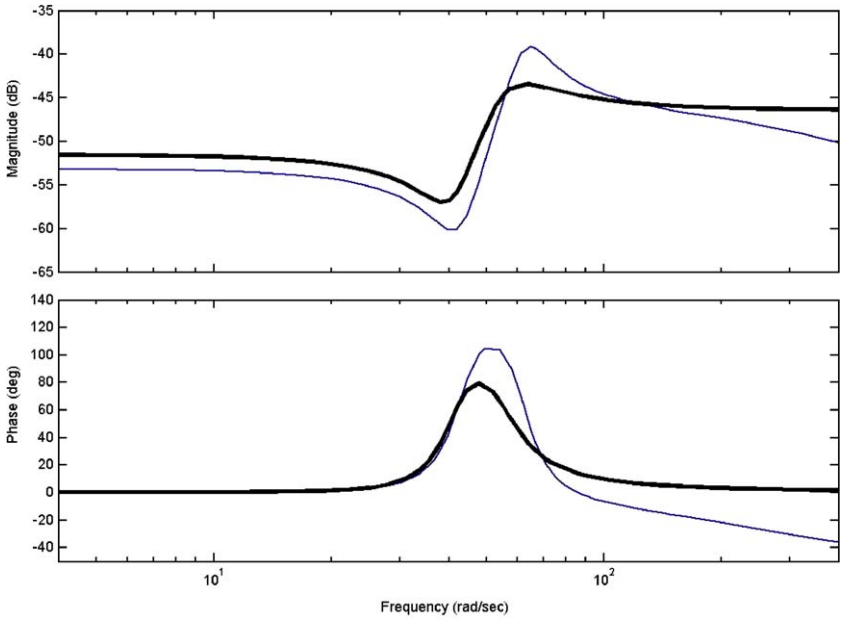

Fig. 11. Experimental data: elements (1,1) of chassis transfer matrix: initial guess (bold line), identified at iteration 2 (thin line).

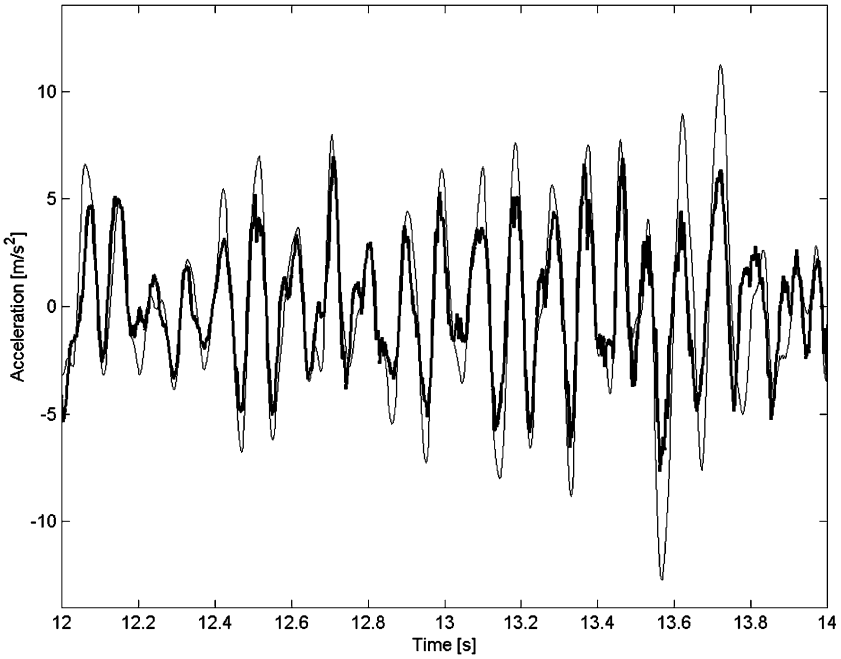

Fig. 12. Experimental data: front chassis accelerations for random road profile and CH Skyhook configuration: measured (bold line), simulated by NSM$^{(1)}$ (thin line).

and NSMS$^{(2)}$ on the testing set are reported. It can be noted that significant improvements in chassis accelerations accuracy have been obtained by means of the second iteration. A third iteration has been also performed, but no significant decrease of errors have been observed.

In Table 4 the RMSE of front and rear chassis accelerations obtained by model NSMS$^{(2)}$ on the testing set are reported for each separate road profile and Skyhook setting.

In Fig. 11 the chassis transfer matrix elements (1,1) of the initial guess and identified at the 2nd iterations are reported.

In Figs. 12–15 measured front and rear chassis accelerations and the ones estimated by models NSMS$^{(1)}$ and NSMS$^{(2)}$ are shown for the portion of testing data corresponding to the last 2 s of the random road profile with the CH Skyhook setting. In Figs. 16 and 17 measured front and rear chassis accelerations and the ones estimated

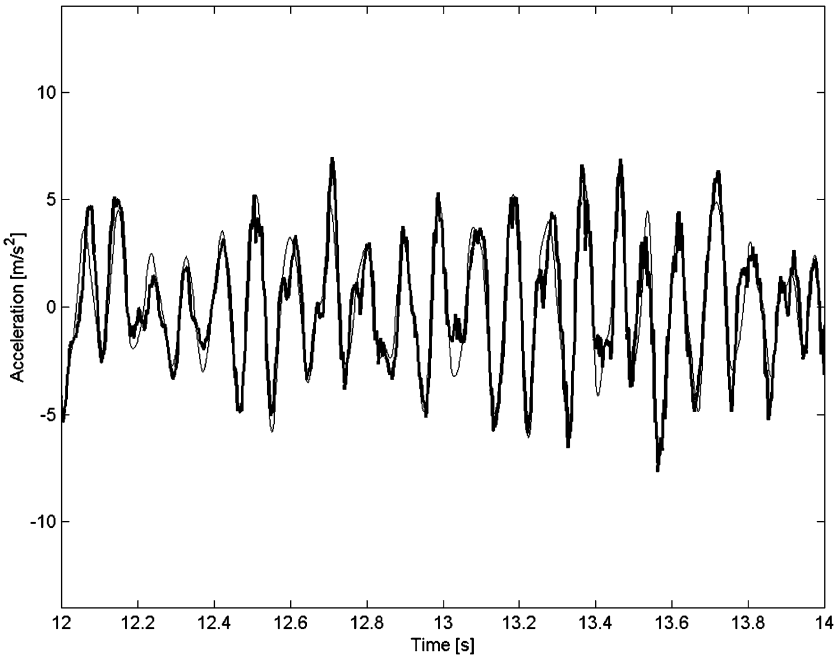

Fig. 13. Experimental data: front chassis accelerations for random road profile and CH Skyhook configuration: measured (bold line), simulated by NSM$^{(2)}$ (thin line).

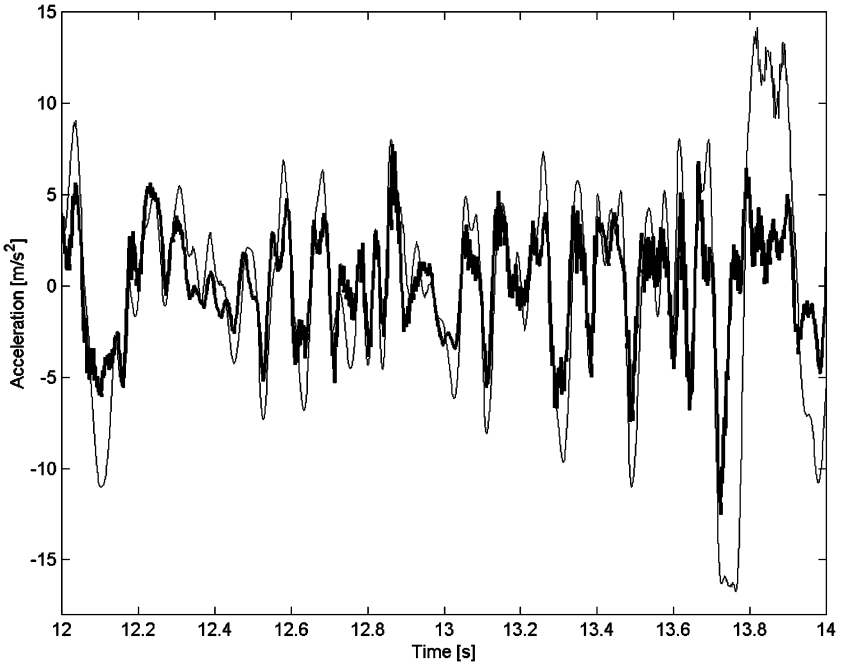

Fig. 14. Experimental data: rear chassis accelerations for random road profile and CH Skyhook configuration: measured (bold line), simulated by NSM$^{(1)}$ (thin line).

by models NSMS$^{(2)}$ are shown for the portion of testing data corresponding to the first second of the English track road profile with the H Skyhook setting.

In conclusion, the identified model NSMS$^{(2)}$ appears to provide quite satisfactory simulation accuracy for all the considered road profiles and Skyhook settings. This can be seen in the tables reporting the simulation RMSEs, which result quite small compared to the amplitudes of the considered accelerations signals, and in all the figures, where the experimental data are simulated with an

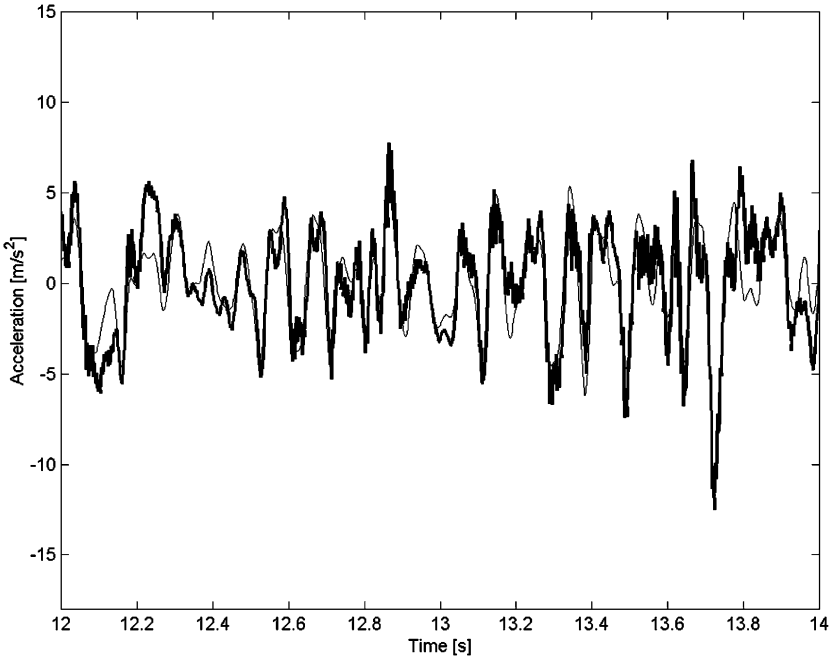

Fig. 15. Experimental data: rear chassis accelerations for random road profile and CH Skyhook configuration: measured (bold line), simulated by NSM$^{(2)}$ (thin line).

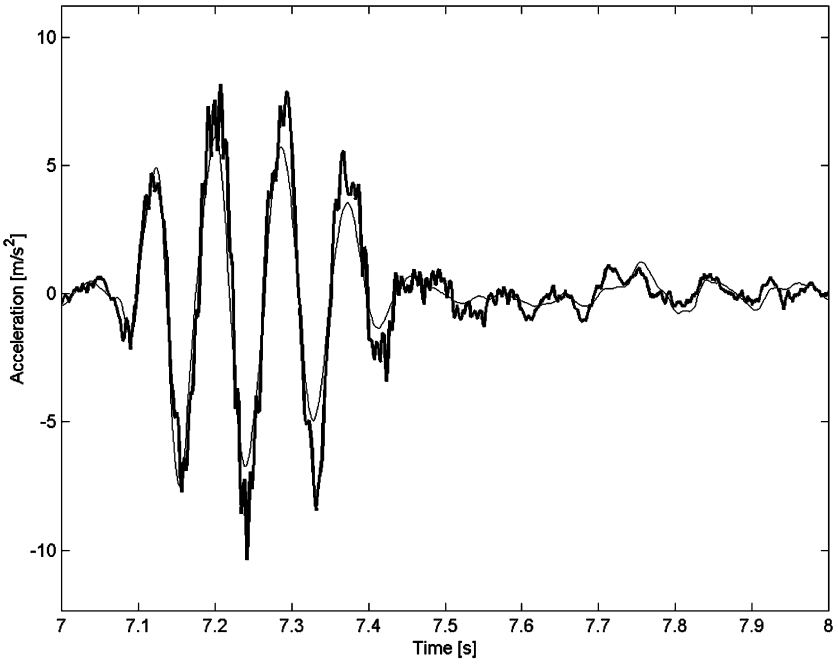

Fig. 16. Experimental data: front chassis accelerations for English track road profile and H Skyhook configuration: measured (bold line), simulated by NSM$^{(2)}$ (thin line).

accuracy which appears to be quite good, especially in view of the fact that a wide range of frequencies is accounted for the model to be used in evaluating the comfort performances of the damper control system. To our knowledge vertical dynamics physical models, even using the most sophisticated physical equations for chassis, suspensions, wheels and tires, do not provide, on the considered frequency range, simulation accuracy comparable to the one provided by the NSMS$^{(2)}$ model.

The NSMS$^{(2)}$ model has been actually used to design and test the fast model predictive control (FMPC) system for vehicles with semi-active suspensions proposed in Canale,

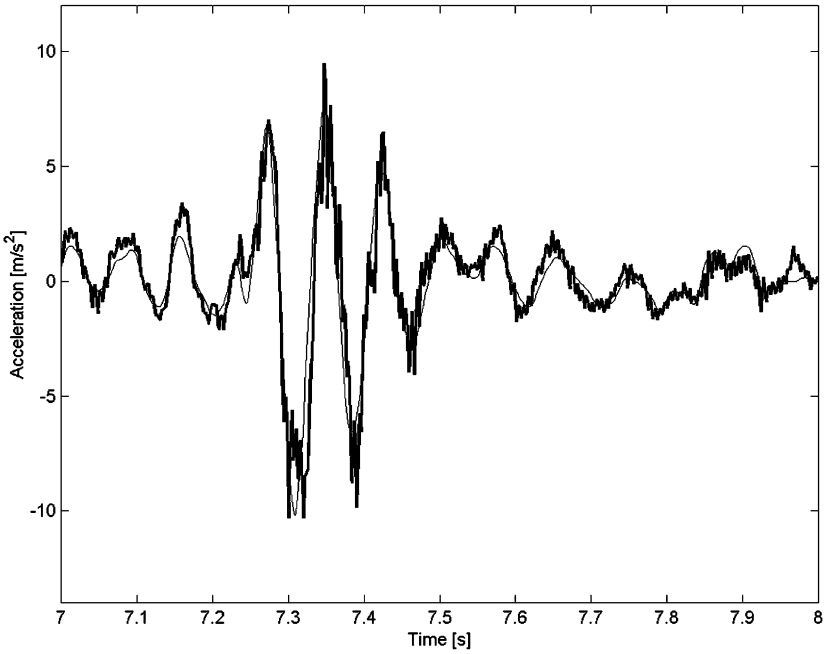

Fig. 17. Experimental data: rear chassis accelerations for English track road profile and H Skyhook configuration: measured (bold line), simulated by NSM$^{(2)}$ (thin line).

Milanese, Novara, and Ahmad (2005) and registered as patent N. PCT/IB2005/000622. The FMPC control system has been tested with success on a real car on a test bench at Centro Ricerche FIAT, largely confirming the simulation results obtained in virtual environment based on the NSMS$^{(2)}$ model.

6. Conclusions

Block-oriented or structured identification is a well known approach used in the literature to face the complexity and accuracy problems in identification of nonlinear systems. In particular, accounting for physical information on the interconnection structure of the system to be identified, significant improvements in identification accuracy over unstructured methods may be obtained. Widely investigated are Hammerstein, Wiener or Lur'e systems, consisting of linear dynamic and nonlinear static systems, connected in cascade or feedback form. However, in practical applications more general decomposition structures may arise, where the nonlinear systems may be dynamic, as shown in the presented example of controlled suspension vehicles. In the paper we have proposed an iterative algorithm for the identification of a system composed of two dynamic MIMO systems, one linear and the other one nonlinear, interconnected in feedback form by an unknown multivariable signal.

A key feature of the proposed structured identification method is that the dynamic nonlinear subsystem is not supposed to have a given parametric form. In this way the complexity/accuracy problems posed by the proper choice of a suitable parametrization and by trapping in local minima during parameters optimization are circumvented. Moreover, the simulation error of the overall model is shown to be a nonincreasing function of iterations. Indeed, the algorithm may converge in few iterations to very satisfactory estimates even for quite rough initializations, as shown in the presented example, related to the identification of the vertical dynamics of vehicles with controlled suspensions.

The results presented here and in Milanese, Novara, Mastronardi, and Amoroso (2004), where the method is applied to a more complex decomposition, show that the proposed structured identification algorithm may prove to give quite accurate models in non trivial real applications.

References

Bai, E. W. (2002). Identification of linear systems with hard input nonlinearities of known structure. *Automatica*, *38*, 853–860.

Bai, E. W. (2003). Frequency domain identification of Wiener models. *Automatica*, *39*, 1521–1530.

Bauer, D., & Ninness, B. (2002). Asymptotic properties of least-squares estimates of Hammerstein–Wiener models. *International Journal of Control*, *75*(1), 34–51.

Billings, S. A., & Tsang, K. M. (1990). Spectral analysis of block structured nonlinear systems. *Mechanical Systems Signal and Processing*, *4*(2), 117–130.

Canale, M., Milanese, M., Novara, C., & Ahmad, Z. (2005). Semi-active suspension control using "fast" model predictive control. In *Proceedings of the 24th American control conference*. Portland, Oregon.

Chen, J., & Gu, G. (2000). *Control-oriented system identification: An H_∞ approach*. New York: Wiley.

Crama, P., & Shoukens, J. (2001). Initial estimate of Wiener and Hammerstein systems using multisine excitation. *IEEE Transactions on Instrumentation and Measurement*, *50*(6), 1791–1795.

Haber, R., & Unbehauen, H. (1990). Structure identification of nonlinear dynamic systems— a survey on input/output approaches. *Automatica*, *26*, 651–677.

Isermann, R., Ernst, S., & Nelles, O. (1997). Identification with dynamic neural networks—architectures, comparisons, applications. In: *Sysid 97* (Vol. 3, pp. 997–1022).

Krtolica, R., & Hrovat, D. (1992). Optimal active suspension control based on a half-car model: An analytical solution. *IEEE Transactions on Automatic Control*, *37*(4), 2238–2243.

Lang, Z. Q. (1997). A nonparametric polynomial identification algorithm for the Hammerstain system. *IEEE Transactions on Automatic Control*, *42*(10), 1435–1441.

Ljung, L., & Caines, P. E. (1979). Asymptotic normality of prediction error estimators for approximate system models. *Stochastics*, *3*, 29–46.

Lu, J., & DePoyster, M. (2002). Multiobjective optimal suspension control to achieve integrated ride and handling performance. *IEEE Transactions on Control Systems Technology*, *10*(6), 807–821.

Milanese, M., & Novara, C. (2003). Model quality in nonlinear SM identification. In *Proceedings of the 42nd IEEE conference on decision and control*. Maui, Hawaii.

Milanese, M., & Novara, C. (2004). Set membership identification of nonlinear systems. *Automatica*, *40/6*, 957–975.

Milanese, M., Norton, J., Piet Lahanier, H., & Walter, E. (1996). *Bounding approaches to system identification*. New York: Plenum Press.

Milanese, M., Novara, C., Mastronardi, F., & Amoroso, D. (2004). Experimental modeling of vertical dynamics of vehicles with controlled suspensions. In *SAE World congress*. Detroit, Michigan.

Narendra, K. S., & Gallman, P. G. (1966). An iterative method for the identification of nonlinear systems using a Hammerstein model. *IEEE Transactions on Automatic Control*, *11*, 546–550.

Narendra, K. S., & Mukhopadhyay, S., (1997). Neural networks for system identification. In *Sysid 97* (Vol. 2. pp. 763–770).

Partington, J. R. (1991). Robust identification and interpolation in H_∞. *International Journal of Control*, *54*, 1281–1290.

Rangan, S., Wolodkin, G., & Poolla, K. (1995). New results for Hammerstein system identification. In *34th conference on decision and control* (pp. 697–702). New Orleans, LA.

Sjöberg, J., Zhang, Q., Ljung, L., Benveniste, A., Delyon, B., Glorennec, P., et al. (1995). Nonlinear black-box modeling in system identification: A unified overview. *Automatica*, *31*, 1691–1723.

Stoica, P. (1981). On the convergence of an iterative algorithm used for Hammerstein system identification. *IEEE Transactions on Automatic Control*, *26*, 967–969.

Vörös, J. (1999). Iterative algorithm for parameter identification of Hammerstein systems with two-segment nonlinearities. *IEEE Transactions on Automatic Control*, *44*(11), 967–969.